Mobility Model for WBANs

M. M. Sandhu[1], M. Akbar[1], M. Behzad[1], N. Javaid[1,2], Z. A. Khan[3], U. Qasim[4]
[1]EE Dept, COMSATS Institute of Information Technology, Islamabad, Pakistan
[2]CAST, COMSATS Institute of Information Technology, Islamabad, Pakistan
[3]Internetworking Program, FE, Dalhousie University, Halifax, Canada
[4]University of Alberta, Alberta, Canada

***Abstract*—Mobility models play a vital role on the accuracy of simulations in Wireless Body Area Networks (WBANs). In this paper, we propose a mobility model for the movement of nodes placed on the human body. During routine activities, body exhibits different postures like standing, sitting, laying, *etc*. We form a mathematical model for the movement of nodes according to the posture pattern. Postures change from one state to another depending upon probabilities. During movement, the distance between nodes and sink is changed which affects the energy consumption of nodes. We implement the proposed mobility model in multi-hop and forwarder based routing techniques and study their performance parameters.**

***Index Terms*—Mobility, WBANs, postures, movement, efficiency, energy, consumption, lifetime, throughput**

I. Introduction

Wireless Body Area Network (WBAN) consists of nodes placed on the human body to monitor different vital signs like heart rate, glucose level, blood oxygen level, *etc*. Mobility models play a vital role on the accuracy of simulations of WBANs. Several mobility models are proposed in literature for wireless sensor networks and ad hoc networks. However, they are not suitable for WBANs due to their different movement pattern. In general, the movement of nodes can be classified into two categories as single and group mobility. In the former case there is no correlation between the movement of different nodes. In this scenario, nodes move regardless the mobility pattern of other nodes in the network. In the latter approach, however, nodes move in a group having a particular relationship between them. In this case, nodes move relative to a reference which decides the movement pattern of other nodes.

In Random Walk Mobility Model (RWMM) [1], nodes randomly select new direction and velocity from a given range. Then the nodes move towards the selected target point. After reaching the target, they select a new direction and speed and the process repeats. The movement of nodes takes place in the bounded simulation area.

In Random Waypoint Mobility Model (RWPM) [2], pause time in introduced between the changes in speed and direction of nodes and it is selected randomly from a given range. In RWPM, a node choses a destination randomly from simulation area and moves towards it at a randomly chosen speed.

In Reference Point Group Mobility Model (RPGM) [3], each group has a centre, which is either a logical centre or group leader node. The movement of group leader determines the mobility behaviour of the entire group.

The rest of paper is organized as follows: section II describes the mobility model while section III shows the energy consumption analysis. Multi-hop and forwarder based routing protocols are detailed in sections IV and V, respectively. Sections VI gives the simulation results and finally conclusion is given in section VII.

II. Mobility Modeling

In WBANs, nodes are deployed on the human body to monitor different physiological parameters, like, blood pressure, temperature, heart beat level, *etc*. These nodes send their sensed data to the sink placed on the chest of the human body. The distances between nodes and sink are constant in static position. However, as the human body is mobile in reality, so, the distance between node and sink changes. In this work, we propose a method to calculate the distances between nodes and sink when the human body is in motion.

We devise a mechanism consisting of two phases, (1) Posture selection phase and (2) Nodes' movement phase. In the posture selection phase, a posture of the human body is selected like, standing, sitting, laying, walking, and running. The probability of posture change can be determined from real human mobility traces. However, we take probabilities of different postures from [4], as shown in fig. 1. Markov chain in the figure shows the probability of posture change from one state to another. After posture change, the new position of nodes is selected in the second phase. We assume that sink is placed on the chest of human body and all positions of nodes are measured relative to it. The following sections discuss the different postures of human body in detail.

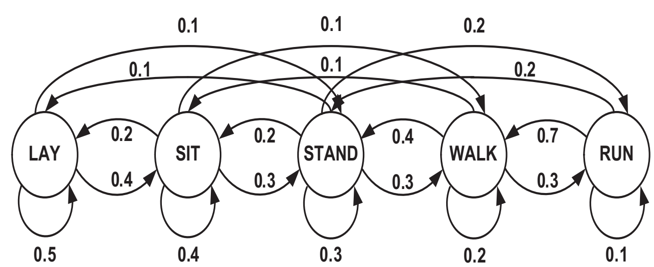

Fig. 1. Markov model for posture pattern selection

A. Standing

In this position, the distances between nodes and sink are constant as body is in static position as shown in fig. 5.

978-1-4799-4173-5/14 $31.00 © 2014 IEEE
DOI 10.1109/BWCCA.2014.60

B. Sitting and Laying

In the sitting and laying postures, we assume that the human body is sitting on a chair and laying on a bed, respectively. In these positions, there is little movement of trunk of the human body. Most of the time, the human arms and legs exhibit motion in three dimensions. We calculate the positions of nodes placed on arms and legs. As nodes placed on arms show similar behaviour, so, we calculate the position of a single node placed on elbow. Similarly, we calculate the position of node placed on knee. The node *e* is placed on the elbow while node *k* is placed on the knee.

The normal position of *e* is given as:

$$P_e = P(\rho_e, \theta_e, \phi_e). \quad (1)$$

Where, ρ_e is the radial distance, θ_e is polar angle and ϕ_e is azimuthal angle of *e* from sink. During movement of the human arm, the maximum and minimum distances between *e* and sink are ρ_{emax} and ρ_{emin}, respectively. So, the difference between these distances is given as:

$$d_e = \rho_{emax} - \rho_{emin}. \quad (2)$$

We form a sphere at distance of $\frac{\rho_{emax}+\rho_{emin}}{2}$ from sink as shown in fig. 2 (*which shows the case for sitting posture*). This sphere has radius of $\frac{d_e}{2}$. Now, during movement, the node *e* will always lie in this sphere. The new position of node *e* is calculated using the following equation.

$$\rho_e(t) = \rho_e(t-1) + (\eta_e \times rand(1) \times \zeta_e). \quad (3)$$

Where, η_e is given as:

$$\eta_e = \begin{cases} [-1 \;\; 0] & \text{if } \rho_e(t) = \rho_{emax}, \\ [0 \;\; 1] & \text{if } \rho_e(t) = \rho_{emin}, \\ [-1 \;\; 1] & \text{if } \rho_{emin} < \rho_e(t) < \rho_{emax}. \end{cases} \quad (4)$$

From eq. 3, it is evident that the new position of a node depends upon the previous position. A random number is added to the current location to find new location. If the new position of node goes out of bound, η_e will decrement the distance between node and center of the sphere (*see eq. 4*).

In eq. 3, ζ_e is the step size which can be adjusted according to the application. Its value is always greater than zero. As the main concern in WBANs is the distance between nodes and sink, so, we will not calculate other parameters like, θ_e and ϕ_e. It should be kept in mind that these values will also change according to eq. 3.

Now, we discuss the movement of node *k* placed on the knee of the human body. The normal position of *k* in sitting position is given as:

$$P_k = P(\rho_k, \theta_k, \phi_k). \quad (5)$$

Here, ρ_k is the normal distance of *k* from sink. θ_k and ϕ_k represent the polar and azimuthal angles, respectively. During movement of human body, the maximum and minimum distances between *k* and sink are denoted by ρ_{kmax} and ρ_{kmin}, respectively.

$$d_k = \rho_{kmax} - \rho_{kmin}. \quad (6)$$

We form a sphere at a distance of $\frac{\rho_{kmax}+\rho_{kmin}}{2}$ from sink as shown in fig. 2. This sphere has radius of $\frac{d_k}{2}$. The node *k* always lie in this sphere during movement. The new position of *k* is calculated using the following equation.

$$\rho_k(t) = \rho_k(t-1) + (\eta_k \times rand(1) \times \zeta_k). \quad (7)$$

The value of η_k is calculated using:

$$\eta_k = \begin{cases} [-1 \;\; 0] & \text{if } \rho_k(t) = \rho_{kmax}, \\ [0 \;\; 1] & \text{if } \rho_k(t) = \rho_{kmin}, \\ [-1 \;\; 1] & \text{if } \rho_{kmin} < \rho_k(t) < \rho_{kmax}. \end{cases} \quad (8)$$

The new position of *k* is calculated using eq. 7 where η_k is a random number which is calculated using eq. 8. ζ_k represents the step size and is adjusted according to the application. Its value is always greater than zero.

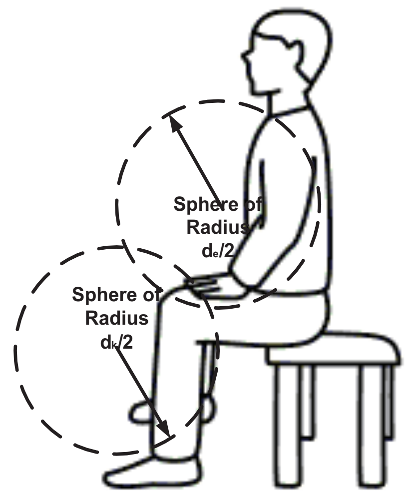

Fig. 2. Human body in sitting position

C. Walking and Running

During walking and running, the arms and legs of human show repetitive and similar trends. When the left arm moves forward, the right leg also moves in the forward direction. This defined trajectory helps to efficiently model the mobility of human body. When the body moves from static position, the new position of sink is given as:

$$P_s = P(\rho_s, \theta_s, \phi_s). \quad (9)$$

Where, ρ_s is calculated as:

$$\rho_s(t) = \rho_o + tu. \quad (10)$$

u denotes the speed of the human and t is the time after which we are calculating new position. Whereas, ρ_o denotes the initial position of sink.

The normal position of node *e* is given as:

$$P_e = P(\rho_e, \theta_e, \phi_e). \quad (11)$$

Let us denote the distances between sink and node in forward and backward positions by ρ_e^{front} and ρ_e^{back}, respectively. We assume that their magnitudes are same. So, we form a curve between ρ_e^{front} and ρ_e^{back} as shown in fig. 3 (*which shows the case for walking posture*). The node *e* moves along this curve and its position at any time *t* is calculated as:

$$\rho_e(t) = \rho_e + \eta_e d_e. \quad (12)$$

Where, d_e is calculated as:

$$d_e = \rho_e^{front} - \rho_e = \rho_e^{back} - \rho_e. \quad (13)$$

The value of η_e changes with time as shown in fig. 4.
Now, we see the movement of nodes placed on legs. The normal position of node *k* is given as:

$$P_k = P(\rho_k, \theta_k, \phi_k). \quad (14)$$

During walking and running, the legs move in the forward and backward directions repeatedly. We denote the distances between sink and node *k* in forward and backward directions by ρ_k^{front} and ρ_k^{back}, respectively. We assume that these two distances are same and form a curve between them as shown in fig. 3. The moving node *k* always lies on this curve. The new position of *k* is calculated as:

$$\rho_k(t) = \rho_k + \eta_k d_k. \quad (15)$$

In the above equation d_k is calculated as:

$$d_k = \rho_k^{front} - \rho_k = \rho_k^{back} - \rho_k. \quad (16)$$

The value of η_k changes with time as shown in fig. 4.

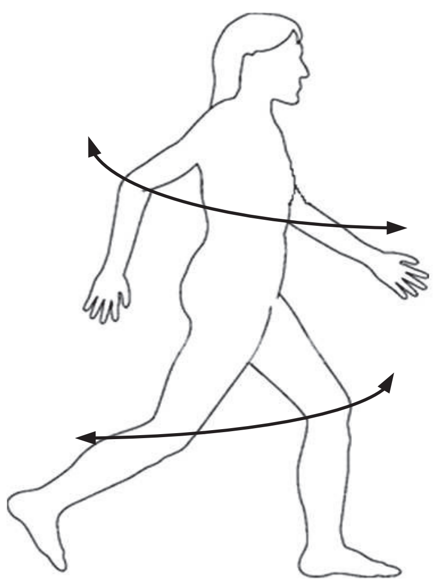

Fig. 3. Human body in walking position

III. Energy Consumption Analysis

Energy consumed in single-hop communication is given as:

$$E_{SH} = E_{TX} \quad . \quad (17)$$

Where, E_{TX} is the transmission energy which is calculated as:

$$E_{TX} = k \times (E_{TXelect} + \varepsilon_{amp}) \times d^2 \quad . \quad (18)$$

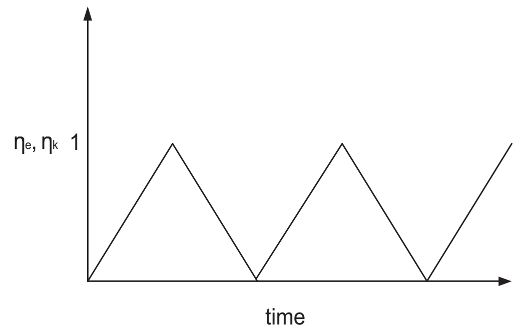

Fig. 4. Value of η_e and η_k

k is packet size, $E_{TXelect}$ is energy consumed by the electronic circuit, ε_{amp} is the amplification energy and d is the distance between transmitter and receiver.
Energy consumed in multi-hop communication is given as:

$$E_{MH} = k \times (h \times E_{TX} + (h-1)(E_{RX} + E_{DA})) \quad . \quad (19)$$

Where, h is the number of hops, E_{RX} is the energy consumed in receiving the data and E_{DA} is the data aggregation energy.

IV. Multi-hop Technique

In multi-hop routing technique, data is transmitted using neighbouring nodes. Fig. 5 shows the placement of nodes on human body. In multi-hop scheme, node 4 sends data to node 1 and node 3 sends data to node 2. Similarly, nodes 7 and 8 send their data to nodes 5 and 6 respectively. The receiving nodes (*i.e.* nodes 1, 2, 5 and 6) send the aggregated data to sink. If these receiving nodes become dead then the other nodes send their data directly to the sink as shown in fig. 6.
In this scheme, the far away nodes send data to their neighboring nodes and thus save energy. However, the drawback of this scheme is that nodes near the sink are burdened with heavy load. They consume extra energy in aggregating and receiving the data from other nodes. In this way, they deplete their energy soon, and become dead nodes.

V. Data Transmission using Forwarder Nodes

In this routing technique, forwarder nodes are selected in each round. These forwarders receive data from their respective group members and forward it to the sink. Fig. 5 shows the placement of nodes on the human body. We discuss this protocol in the following sections in detail.

A. Initialization phase

In this phase, sink broadcasts a HELLO message containing the following information:

- Location of sink.
- Location of neighbors.
- Information about all possible routes to the sink.

All nodes receive this HELLO message and update their routing table.

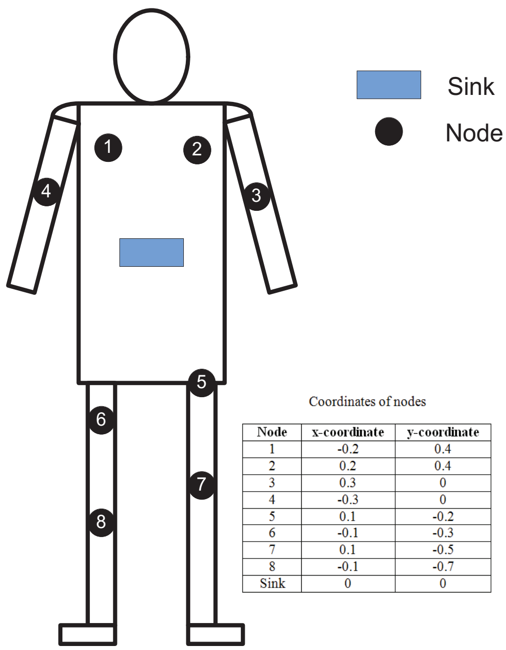

Node	x-coordinate	y-coordinate
1	-0.2	0.4
2	0.2	0.4
3	0.3	0
4	-0.3	0
5	0.1	-0.2
6	-0.1	-0.3
7	0.1	-0.5
8	-0.1	-0.7
Sink	0	0

Fig. 5. Placement of nodes on the human body

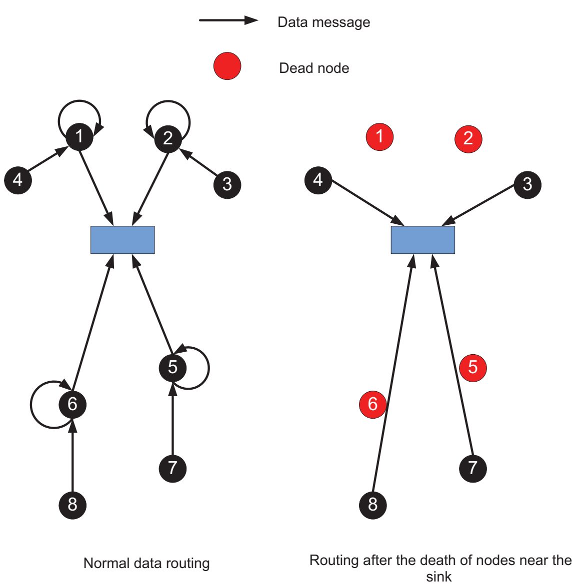

Fig. 6. Network flow tree in multi-hop routing scheme

B. Forwarders' selection phase

In this phase, forwarders are selected to route the data of other nodes. We divide N number of nodes into two sets; A and B, based on their distance from sink, which are given as:

$$N = \{1, 2, 3, 4, 5, 6, 7, 8\} \tag{20}$$

$$A = \{1, 2, 3, 4\} \tag{21}$$

$$B = \{5, 6, 7, 8\} \tag{22}$$

In the forwarders' selection phase, two forwarder nodes are selected (*one from each group*) on the basis of cost functions $C.F_A$ and $C.F_B$, which are calculated as:

$$C.F_A = \frac{d(i)}{R.E(i)}. \quad i \in A \tag{23}$$

$$C.F_B = \frac{d(i)}{R.E(i)}. \quad i \in B \tag{24}$$

The node having minimum value of $C.F_A$ is selected as a forwarder node from group A. Similarly, the node having minimum value of $C.F_B$ is selected as forwarder node from group B. These forwarder nodes collect the data from their respective group members and send it to the sink.

C. Scheduling phase

In the scheduling phase, forwarders assign Time Division Multiple Access (TDMA) based time slots to their children nodes. All the nodes transmit in their scheduled time slots to avoid collision.

D. Data transmission phase

In the data transmission phase, nodes transmit data to their respective forwarder nodes in their scheduled time slots. Forwarder nodes receive data from their children nodes, aggregate it and route it to the sink. If a node has less energy than a threshold (τ), it does not take part in forwarders' selection and routes its data directly to the sink. This is incorporated to save the data aggregation energy of low energy nodes. If a node has less distance to the sink than forwarder then it routes its data directly to the sink. Fig. 7 shows the network flow tree for forwarder based routing technique. In the initial rounds, nodes send data to their respective forwarders which route it to the sink. However, after some rounds, some nodes may have less energy than other as shown in fig. 7. For example, if node 5 has less energy than τ, it sends its data directly to the sink. Other nodes route their data through forwarder nodes.

VI. Simulation Results and Analysis

We simulate the proposed protocols and analyze their results. Table I shows the simulation parameters and their values. We implement the proposed mobility model in the two routing protocols and assume the values of ρ_e and ρ_k as 0.15 and 0.20 respectively. We ignore the sensing energy consumed by the nodes in simulation. The initial energy (E_o) of all nodes is 0.5 J. The simulations are run five times and their average results are plotted.

A. Stability period and network lifetime

Network lifetime represents the time from the start of network till the death of last node. On the other hand, the time from start of the network till the death of first node is called stability period. Fig. 8 shows the comparison of number of dead nodes and fig. 9 shows the comparison of stability period and network lifetime. Forwarders based routing protocol has larger stability period and network lifetime. It is due to the fact that new forwarders are selected in each round and the

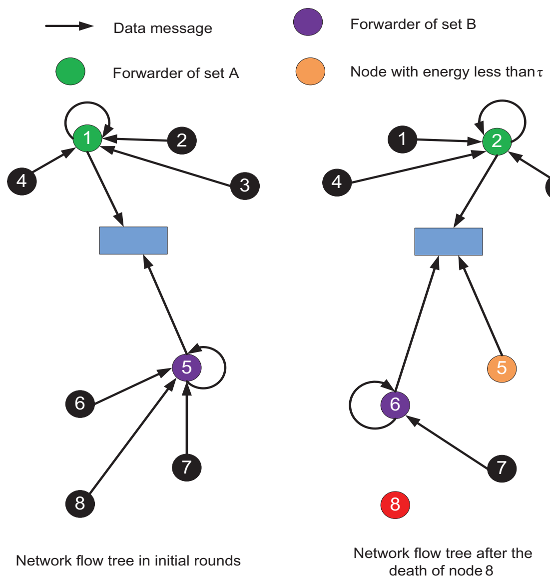

Fig. 7. Network flow tree in forwarder based routing scheme

TABLE I
SIMULATION PARAMETERS

Parameter	Value	Units
$E_{RXelect}$	36.1	nJ/bit
$E_{TXelect}$	16.7	nJ/bit
ε_{amp}	1.97	nJ/bit/m^2
E_{DA}	5	nJ/bit/signal
d_o	0.1	m
τ	0.2	J
k	4000	bits
f	2.4	GHz
E_o	0.5	J

load is uniformly distributed to all the nodes. On the other hand, in multi-hop routing protocol, nodes near the sink are heavily burdened and consume more energy in the form of reception and data aggregation energy. As a result, these nodes die quickly. Multi-hop routing protocol has stability period of 1191 rounds and network lifetime of about 2500 rounds. On the other hand, forwarders based routing scheme has stability period of 3913 rounds and network lifetime of 6878 rounds as shown in fig. 9.

B. Throughput

Throughput shows the number of packets successfully received at sink. A protocol having longer network lifetime sends more packets to the sink and have higher throughput. Fig. 10 shows the number of packets sent to the sink in the multi-hop and forwarders based routing protocols. As forwarders based routing protocol has longer network lifetime (*see fig. 9*), so, it sends more packets to the sink. All of the sent packets are not successfully received at sink. We use Random Uniformed Model [7] to calculate the number of dropped and received packets. The status of the communication link can be good or bad. We assume the probability of 0.7 for link to be good. Figs. 11 and 12 show the number of packets dropped and

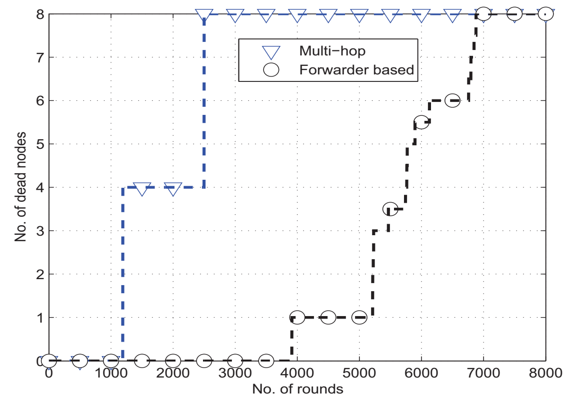

Fig. 8. Comparison of number of dead nodes

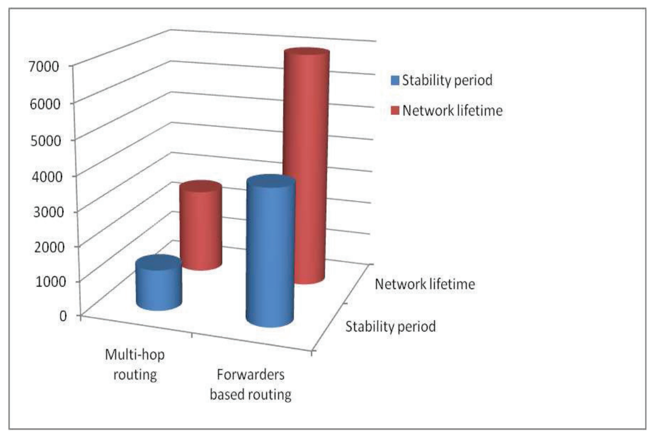

Fig. 9. Comparison of stability period and network lifetime

successfully received at sink, respectively. It is evident from fig. 12 that multi-hop routing technique continuously sends packets to sink till 2500 rounds whereas forwarders based routing technique sends packets to the sink till 6878 rounds.

C. Residual energy

Comparison of residual energy of the multi-hop and forwarders based routing protocols is shown in fig. 13. As nodes near the sink consume more energy in multi-hop routing, so, they deplete their energy soon. On the other hand, nodes in the forwarder based routing protocol consume less energy and stay alive for longer time. Fig. 13 shows the gradual decrease in the residual energy of forwarder based routing protocol. Whereas, in the multi-hop routing protocol the residual energy decreases more quickly.

VII. CONCLUSION

We propose a mobility model for the movement of nodes placed on the human body in WBAN. First of all, a posture is selected according to a probability and then the nodes move according to the selected posture. During movement, the distance between sink and nodes is changed which affects

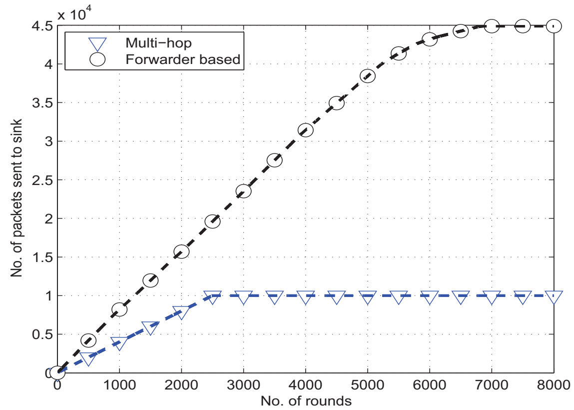

Fig. 10. Comparison of packets sent to sink (aggregated)

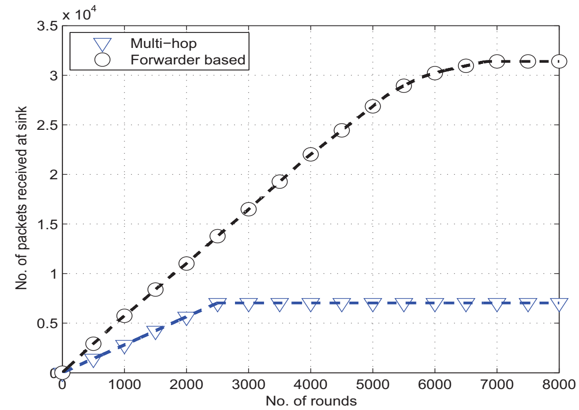

Fig. 12. Comparison of received packets (aggregated)

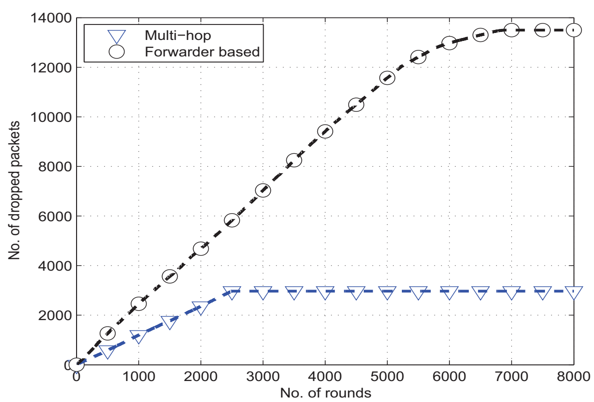

Fig. 11. Comparison of dropped packets (aggregated)

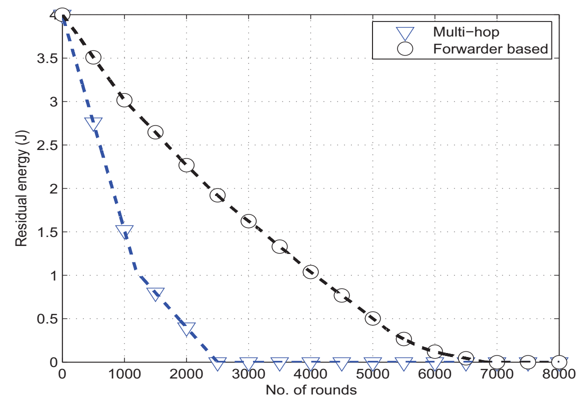

Fig. 13. Comparison of residual energy

the energy consumption, network lifetime, and throughput. We implement the proposed mobility model in multi-hop and forwarder based routing techniques and study their performance parameters. Simulation results show that forwarder based routing technique has increased network lifetime, stability period and throughput.

In future, we will implement the proposed technique on real experimental test bed.

REFERENCES

[1] Zonoozi, Mahmood M., and Prem Dassanayake. "User mobility modeling and characterization of mobility patterns." Selected Areas in Communications, IEEE Journal on 15.7 (1997): 1239-1252.

[2] Hyyti, Esa, and Jorma Virtamo. "Random waypoint mobility model in cellular networks." Wireless Networks 13.2 (2007): 177-188.

[3] Hong, Xiaoyan, et al. "A group mobility model for ad hoc wireless networks." Proceedings of the 2nd ACM international workshop on Modeling, analysis and simulation of wireless and mobile systems. ACM, 1999.

[4] Nabi, Majid, Marc Geilen, and Twan Basten. *"MoBAN: A configurable mobility model for wireless body area networks."* Proceedings of the 4th International ICST Conference on Simulation Tools and Techniques. ICST (Institute for Computer Sciences, Social-Informatics and Telecommunications Engineering), 2011.

[5] Heinzelman, Wendi Rabiner, Anantha Chandrakasan, and Hari Balakrishnan. "Energy-efficient communication protocol for wireless microsensor networks." System Sciences, 2000. Proceedings of the 33rd Annual Hawaii International Conference on. IEEE, 2000.

[6] Reusens, Elisabeth, et al. "Characterization of on-body communication channel and energy efficient topology design for wireless body area networks." Information Technology in Biomedicine, IEEE Transactions on 13.6 (2009): 933-945.

[7] Zhou, Qili, et al. "A solution to error and loss in wireless network transfer." Wireless Networks and Information Systems, 2009. WNIS'09. International Conference on. IEEE, 2009.

[8] Reusens, Elisabeth, et al. "Characterization of on-body communication channel and energy efficient topology design for wireless body area networks." Information Technology in Biomedicine, IEEE Transactions on 13.6 (2009): 933-945.